

1 **The role of internal nitrogen loading in supporting non-N-fixing harmful cyanobacterial**
2 **blooms in the water column of a large eutrophic lake**

3 Daniel K. Hoffman¹, Mark J. McCarthy², Ashlynn R. Boedecker³, Justin A. Myers², Silvia E.
4 Newell²

5
6 Running head: Internal N loading supports cyanoHABs in large lakes

7
8 Corresponding Author: Daniel K. Hoffman: dhoffma5@kennesaw.edu

9 ¹Kennesaw State University
10 Department of Ecology, Evolution, and Organismal Biology
11 Kennesaw, GA 30144, USA

12
13 Silvia Newell: silvia.newell@wright.edu

14 Mark McCarthy: mjm.kingston@gmail.com

15 Justin Myers: justin.myers@wright.edu

16 ²Wright State University
17 Department of Earth and Environmental Sciences
18 3640 Colonel Glenn Hwy

19 Dayton, OH 45435, USA

20
21 Ashlynn Boedecker: ashlynn_boedecker2@baylor.edu

22 ³Baylor University
23 Department of Biology

24 One Bear Place
25 Waco, TX 76798, USA

26

27 Keywords: Lake Erie, harmful cyanobacterial blooms, ammonium, internal loading

28

29 **Abstract**

30 Western Lake Erie cyanobacterial harmful algal blooms (cyanoHABs) occur every summer as a
31 result of anthropogenic nutrient loading. While the physiological importance of nitrogen (N) in
32 supporting bloom biomass and toxin production is established, the role of internal N recycling in
33 the water column to support bloom maintenance is lacking. Over three field seasons (2015–
34 2017), we collected water from western Lake Erie and employed bottle incubations with ¹⁵N-
35 ammonium (NH₄⁺) enrichments to determine NH₄⁺ regeneration and potential uptake rates in the
36 water column. Potential NH₄⁺ uptake rates followed spatial and seasonal patterns, with greatest
37 rates measured nearest the Maumee River inflow and during peak bloom months (August and
38 September). Regeneration followed a similar spatial pattern but was greatest in early summer
39 (June and July) and supported ~20–60% of potential NH₄⁺ demand during the height of the
40 bloom. Basin-wide internal NH₄⁺ regeneration during the April–October period could supply
41 NH₄⁺ at 60–200% of annual external N loading to the western basin. These results help explain
42 how non-N-fixing cyanoHABs in Lake Erie, and other large, eutrophic lakes, continue producing
43 biomass and N-rich toxins long after spring nutrient loads are exhausted or transported to other
44 areas. Internal N loads are ultimately driven by external N loads; in low precipitation years,
45 external nutrient loads result in smaller blooms, producing less substrate for subsequent internal

46 N loads. Overall, these findings, along with others, confirm that both internal N loading and
47 external N loading must be considered when evaluating cyanoHAB management strategies.

48

49 **Introduction**

50 *Microcystis*-dominated cyanobacterial harmful algal blooms (cyanoHABs) in western
51 Lake Erie have increased in severity since the mid-1990s (Steffen et al. 2014). Research on and
52 management of high nutrient loads from agricultural watersheds have focused on phosphorus (P)
53 as the key driver of cyanoHABs in Lake Erie (e.g., Martin et al. 2021) and globally (Paerl et al.
54 2016). Although total P and total nitrogen (N) loads have decreased in recent decades, the
55 proportion of dissolved reactive P in the total P load to Lake Erie has increased and correlates
56 with annual bloom size (Jarvie et al. 2017, but see River and Richardson 2019). Likewise, the
57 fraction of the total N (TN) load comprised of chemically reduced N forms (as total Kjeldahl N;
58 TKN) delivered to western Lake Erie has increased concurrently and is also related to
59 cyanoHAB biomass (Newell et al. 2019).

60 Uncertainties in dissolved reactive P analyses related to nanoparticulate P passing
61 through 0.45 μm filters may result in over-estimation of Maumee River fluxes to western Lake
62 Erie by ~50% (River and Richardson 2019). The temporal disconnect, exceeding the basin
63 residence time, between spring dissolved reactive P loads and cyanoHABs in late summer is also
64 problematic (Newell et al. 2019). In contrast, higher TKN (including highly bioavailable
65 ammonium (NH_4^+) and urea) proportions in the Maumee River TN load in mid-summer coincide
66 well with cyanoHAB initiation in July (Newell et al. 2019). Cyanobacteria, particularly non-N
67 fixing taxa, are excellent at scavenging NH_4^+ and often outcompete eukaryotic organisms (e.g.,
68 diatoms) for NH_4^+ (Blomqvist et al. 1994). *Microcystis* and many other toxin-producing, bloom-

69 forming taxa (e.g., *Planktothrix*) cannot fix atmospheric dinitrogen (N₂) and thus rely on
70 combined N, particularly NH₄⁺, in the water column (Paerl et al. 2016). Maximum uptake rates
71 (V_{max}) for NH₄⁺ are 4–6 times greater than those for nitrate (NO₃⁻) in *Microcystis* (Takamura et
72 al. 1987), while diatoms are often more competitive for NO₃⁻ (Glibert et al. 2016).

73 Microcystin and biomass concentrations in non-N fixing cyanobacteria increase in
74 response to NH₄⁺ additions (Chaffin et al. 2018), and NH₄⁺ and urea induce upregulation of
75 microcystin-associated genes (Harke et al. 2016) more quickly than NO₃⁻ (Chaffin et al. 2018).
76 Conversely, low NH₄⁺ concentrations inhibit toxin production due to *ntcA* (global cyanobacteria
77 N regulation gene) activation, the product of which binds to the *mcy* gene cassette responsible for
78 microcystin production and represses its activity (Kuniyoshi et al. 2011). NH₄⁺ bioactivity
79 leads to rapid assimilation and recycling within the sediments and water column, making it
80 difficult to accurately characterize in situ NH₄⁺ concentrations (McCarthy et al. 2013). Thus,
81 snapshot sampling and monitoring efforts for NH₄⁺ concentrations cannot accurately estimate
82 NH₄⁺ availability in situ, which requires measuring NH₄⁺ assimilation and turnover/recycling
83 rates (Gardner et al. 2017).

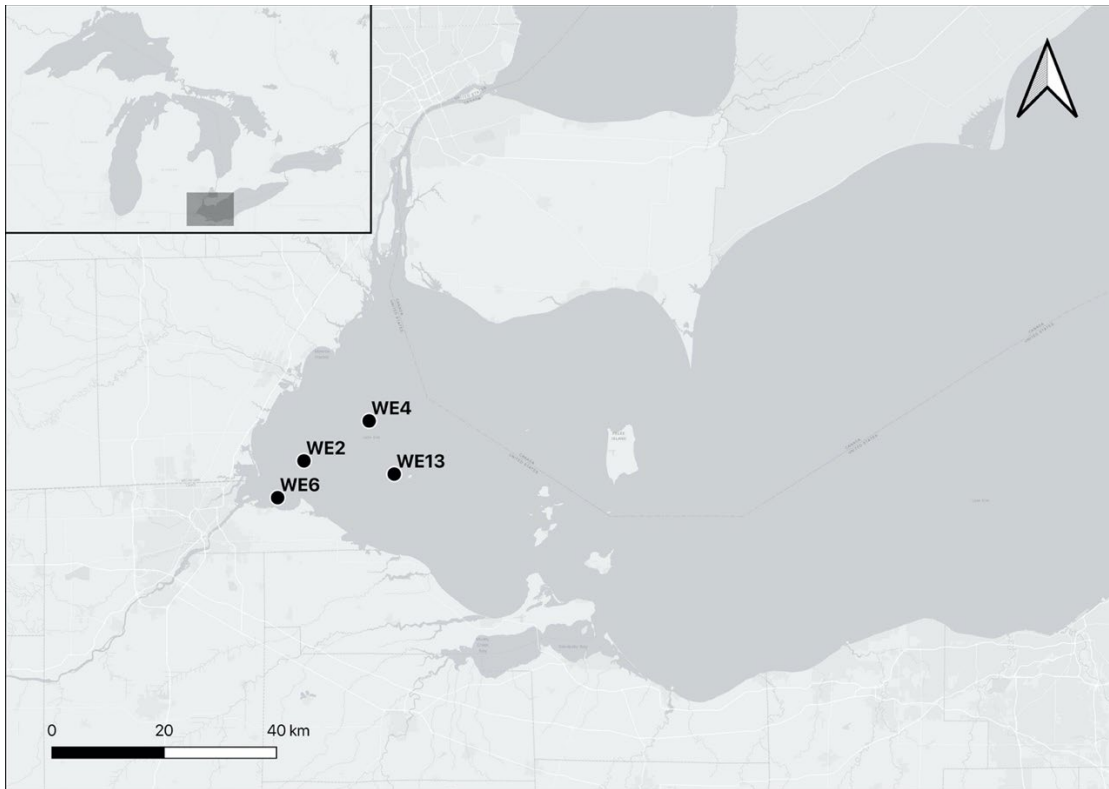
84 Over three field seasons (April through October, 2015–2017), NH₄⁺ regeneration and
85 potential uptake rates were quantified in the western Lake Erie water column to evaluate the
86 importance of internal N loading in supporting non-N-fixing cyanoHAB biomass and toxin
87 production. Potential NH₄⁺ uptake includes both assimilation into primary producer biomass and
88 nitrification (conversion of NH₄⁺ to NO₃⁻). NH₄⁺ regeneration includes, but is not limited to,
89 remineralization of organic compounds, microplankton excretions (including algal exudation),
90 and sloppy feeding by grazers (Hopkinson et al. 1987). We also evaluated the capacity of NH₄⁺

91 regeneration to support water column NH_4^+ demand across the bloom season relative to external
92 TN loading.

93 We expected that NH_4^+ regeneration and potential uptake rates would follow patterns
94 described previously (i.e., photic exceeding dark NH_4^+ uptake, highest NH_4^+ uptake during peak
95 blooms, potential NH_4^+ uptake exceeding regeneration) and follow spatial and temporal trends
96 consistent with seasonality and distance from nutrient sources. Specifically, we hypothesized
97 that: (1) both NH_4^+ regeneration and potential uptake rates would decrease with distance from
98 the Maumee River mouth; (2) both NH_4^+ regeneration and potential uptake rates would increase
99 from late spring/early summer to August and September (peak bloom); and (3) rates measured in
100 near-surface waters would be greater than those from near-bottom waters. We anticipated that
101 the proportion of internal NH_4^+ regeneration capable of supporting potential NH_4^+ uptake would
102 increase throughout from bloom initiation to bloom peak. Given the importance of NH_4^+ to the
103 metabolic demands of cyanoHABs and the difficulty of accurately determining in situ NH_4^+
104 concentrations, quantifying these NH_4^+ cycling pathways is critical to understanding and
105 managing non-N-fixing cyanoHABs in western Lake Erie and other large eutrophic lakes. These
106 kinds of measurements are exceedingly rare in the Great Lakes and other freshwater systems but
107 are critically needed for informing and validating ecosystem models and management actions.

108 **Materials**

109 **Field sampling**



110

111 Figure 1. Western Lake Erie sampling stations. Stations are located at the following coordinates
112 (latitude, longitude): WE6 (41.70555, -83.386533), WE2 (41.7638, -83.330617), WE4
113 (41.8269833, -83.192117), and WE13 (41.7429167, -83.138783).

114

115 Water samples were collected in conjunction with the NOAA Great Lakes Environmental
116 Research Laboratory (GLERL) weekly HABs monitoring program in 2015, 2016, and 2017.

117 Further details on bloom severity, initiation, and duration are presented in supplemental material.

118 Three stations (WE6, WE2, WE4; Fig. 1) were sampled monthly from June–September 2015

119 (Table S1), and these plus WE13 (Fig. 1) were sampled in 2016 and 2017 during May–October

120 (with an additional sampling at WE2 in April 2016). These stations represent a spatial and depth

121 gradient moving away from the Maumee River inflow. Not all stations were sampled during each

122 month, and sampling varied across years due to opportunity and weather constraints, particularly

123 in 2016, when frequent storms interrupted scheduled sampling events. At each station, water was
124 collected from two depths (~1 m below the surface and ~1 m above the sediment-water interface)
125 with a 5-L Niskin bottle. 10 L of water was collected from each depth and transferred into 20-L
126 polyethylene carboys. 12 ml ambient nutrient (orthophosphate (o-PO₄³⁻), NH₄⁺, urea, nitrite
127 (NO₂⁻), NO₃⁻) samples were filtered immediately on-site (0.22 μm Nylon filters) into 15-ml
128 polypropylene sample tubes and frozen in the field (dry ice) until transfer into a -20 °C lab
129 freezer. Other biological and physicochemical parameters (water temperature, dissolved oxygen
130 (DO), total P, Secchi depth, conductivity, photosynthetically active radiation (PAR), turbidity,
131 total suspended solids, and chlorophyll *a*, phycocyanin, and microcystin concentrations) were
132 collected from surface waters and analyzed by NOAA GLERL and CIGLR (NOAA Great Lakes
133 Environmental Research Laboratory; Cooperative Institute for Great Lakes Research, University
134 of Michigan, 2019). All physicochemical data other than nutrients are available in Supplemental
135 Information. The N and P mass of Maumee River loads was obtained from the National Center
136 for Water Quality Research (NCWQR) database, and other ambient environmental
137 characteristics of interest (average daily wind speed, wind direction, air temperature) were
138 selected from buoy data hosted by NOAA's National Data Buoy Center
139 (<https://www.ndbc.noaa.gov>; last accessed 11/30/2020) and Michigan Technological
140 University's Upper Great Lakes Observing System (UGLOS; <http://uglos.mtu.edu>; last accessed
141 11/30/2020).

142 **Incubations**

143 NH₄⁺ regeneration and potential uptake rates were quantified via enrichment with ¹⁵N-
144 labeled NH₄⁺ (McCarthy et al. 2013). 1-L aliquots of water from each station and depth were
145 amended with ¹⁵NH₄Cl (98 atom % ¹⁵N, Sigma Aldrich; final concentration 8–24 μM, depending

146 on sampling date and bloom conditions; Table S1), mixed, and distributed among six clear,
147 colorless, 125 ml Nalgene bottles for triplicate light and dark (foil-wrapped) incubations. Initial
148 samples from each bottle were collected immediately using a syringe and canula, filtered (0.22
149 μm), and frozen at $-20\text{ }^{\circ}\text{C}$ until analysis. Bottles were incubated in a mesh bag for 16–25 hours
150 (Table S1) in simulated ambient lake conditions (outdoor water bath, not temperature-controlled)
151 before being filtered (0.22 μm) into 15-ml polypropylene sample tubes and immediately frozen
152 at $-20\text{ }^{\circ}\text{C}$ until total NH_4^+ analysis ($^{14}\text{N} + ^{15}\text{N}$). Pre- and post-incubation samples for $^{15}\text{NH}_4^+$
153 analyses were filtered into 12-ml Exetainers (Labco) with no headspace, sealed with double-
154 wadded septa caps, and stored in the dark at room temperature ($17\text{ }^{\circ}\text{C}$) until analysis (within one
155 week).

156 **Sample analysis and rate calculations**

157 Total NH_4^+ concentrations were determined via colorimetric flow-injection analysis
158 (Lachat Quikchem 8500). $^{15}\text{NH}_4^+$ concentrations were quantified via OX-MIMS (Yin et al.
159 2014). Additional details on OX-MIMS are provided in supplemental material. Total NH_4^+
160 concentrations were used to determine the $^{15}\text{NH}_4^+$ to total NH_4^+ ratio for use in isotope dilution
161 models (Blackburn 1979; Caperon et al. 1979). Potential NH_4^+ uptake rates were qualified as
162 potential rates due to saturating-level isotope additions (McCarthy et al. 2013), but rates
163 determined from saturating-level isotope amendments tend to converge with actual rates in
164 highly productive aquatic systems (Glibert et al. 1988).

165 In August 2015, $^{15}\text{NH}_4^+$ was undetectable after 21 hours of incubation. However, a clear
166 decrease (up to 50%) in $^{15}\text{NH}_4^+$ concentration was observed between the known amendment and
167 initial sampling ($\sim 15\text{ min}$). Therefore, we calculated NH_4^+ regeneration and potential uptake
168 rates for the abbreviated period. Rates for one station near WE6 were measured from a separate

169 sampling event five days prior to the others, and these data are included in the Supplemental
170 Materials and briefly mentioned in the Discussion, but not included in any statistical analyses.

171 **Statistical analyses**

172 All analyses were performed in R (version 3.6.1; R Core Team 2020). Rate data were
173 visually examined for assumptions of normality and heteroscedasticity and via Shapiro-Wilk
174 tests; all failed to meet normality assumptions, so they were log-transformed prior to analysis.
175 All linear models were conducted with the *lm* function from the “lme4” package (Bates et al.
176 2015). Differences among treatment means were determined via Tukey’s HSD post hoc tests
177 using the *emmeans* function from the “emmeans” package (Lenth et al. 2019). More detail about
178 linear models can be found in Supplemental Information.

179 Spearman’s Rank correlations were calculated using the *rcorr* function from “Hmisc”
180 package (Harrell 2019) to inform relationships between NH_4^+ regeneration and potential uptake
181 and environmental variables. For correlations we added bloom day, defined as days plus or
182 minus the bloom initiation day (as determined by the first report of cyanobacteria in NOAA
183 GLERL HABs bulletins), as a variable.

184

185

186

187

188

189

190

191 **Results**

192 **Ambient conditions**

193 Table 1. Nutrient concentrations ($\mu\text{mol N or P L}^{-1}$) for ammonium (NH_4^+), nitrite (NO_2^-), nitrate
 194 (NO_3^-), orthophosphate (o-PO_4^{3-}), and urea near the water surface. BDL = below method
 195 detection limit.

Date	Station	NH_4^+ (μM)	NO_2^- (μM)	NO_3^- (μM)	o-PO_4^{3-} (μM)	Urea (μM)
22-Jun-15	WE6	7.01	1.21	260	4.10	2.71
	WE2	4.03	0.320	315	1.31	1.35
	WE4	0.646	0.120	22.0	0.040	1.18
20-Jul-15	WE6	5.36	1.93	196	4.19	2.71
	WE2	1.45	2.17	216	3.27	1.44
	WE4	BDL	1.58	49.5	0.040	0.692
10-Aug-15	WE6	BDL	0.740	91.2	0.510	0.470
	WE2	BDL	0.730	99.0	1.21	0.310
	WE4	BDL	0.260	4.98	0.050	0.310
28-Sep-15	WE6	0.650	BDL	0.032	5.56	0.500
	WE2	4.86	BDL	0.024	20.7	0.500
	WE4	0.300	BDL	0.014	6.92	1.50
19-Apr-16	WE2	4.21	0.730	45.6	0.170	0.450
30-May-16	WE4	1.72	BDL	9.50	0.050	0.600
	WE13	6.04	0.370	15.1	0.600	0.400
27-Jun-16	WE6	9.72	1.57	48.8	1.35	2.08
	WE2	5.49	0.500	26.1	0.280	0.560
	WE4	0.54	0.410	11.9	0.010	0.410
11-Jul-16	WE6	0.250	7.40	326	0.080	0.650
	WE2	2.10	0.870	30.6	0.130	0.390
	WE4	0.670	0.560	18.0	0.060	0.250
8-Aug-16	WE6	0.020	0.130	4.97	0.060	0.490
	WE2	0.420	0.570	12.1	0.040	0.300
	WE4	BDL	0.790	8.84	0.050	0.570
	WE13	0.840	0.200	5.40	0.070	1.30
19-Sep-16	WE6	0.800	0.510	9.49	0.790	2.10
	WE2	2.41	0.710	5.78	0.890	0.770
17-Oct-16	WE4	1.86	0.430	19.0	0.570	0.470
	WE13	0.950	2.56	7.82	1.13	0.560
	WE6	1.87	0.650	29.5	0.800	1.20
	WE2	0.430	0.740	20.0	0.380	0.360
30-May-17	WE6	6.48	4.88	373	4.51	2.86
	WE2	2.87	4.85	314	2.65	2.26
	WE4	4.63	0.290	34.2	0.030	0.355
	WE13	1.88	0.450	36.8	0.040	0.423
12-Jun-17	WE6	7.30	4.94	352	4.10	2.71
	WE2	1.55	3.63	230	1.31	1.35
	WE4	2.75	0.540	40.0	0.040	1.18
	WE13	2.11	0.270	33.4	0.040	0.553
17-Jul-17	WE6	6.29	5.13	400	4.32	2.71
	WE2	2.55	5.38	364	2.89	1.44
	WE4	2.52	1.10	42.6	0.080	0.692
	WE13	0.760	0.860	37.5	0.090	0.501
14-Aug-17	WE6	0.330	1.46	122	0.530	0.820
	WE2	0.290	0.450	34.8	0.060	0.722
	WE4	0.720	1.65	77.0	0.090	0.446
	WE13	0.800	1.00	51.4	0.030	0.368
18-Sep-17	WE6	0.270	BDL	0.390	0.040	0.536
	WE2	BDL	0.020	0.700	0.063	0.290
	WE4	0.290	1.19	18.9	0.038	0.345
	WE13	0.260	0.030	0.990	0.039	0.424
10-Oct-17	WE6	BDL	0.020	0.390	0.170	0.539
	WE2	0.040	0.050	0.450	0.210	0.340
	WE4	0.630	0.720	20.7	0.180	0.326
	WE13	0.150	0.480	15.7	0.060	0.219

196

197 NH_4^+ concentrations peaked in June and decreased through the bloom season (Table 1),
198 also decreasing along the distance gradient from the river input. $\text{NO}_3^- + \text{NO}_2^-$ (NO_x)
199 concentrations were usually 5–65 times greater than NH_4^+ and followed a similar spatial trend,
200 with peak NO_x concentrations observed near the Maumee River discharge. NO_x concentrations
201 generally peaked later than NH_4^+ concentrations before decreasing to less than $1 \mu\text{M}$ at the
202 westernmost stations late in the sampling season. Urea concentrations followed similar patterns
203 to those for NH_4^+ , with higher concentrations in June decreasing through the sampling season. o-
204 PO_4^{3-} concentrations in the westernmost part of the basin decreased from mid-summer until
205 bloom initiation. High o- PO_4^{3-} concentrations ($5\text{--}20 \mu\text{M}$) were observed in surface waters in
206 September 2015, despite most N forms being depleted. o- PO_4^{3-} concentrations in 2016 did not
207 exhibit the decreasing trend observed in the other two years.

208

209

210

211

212

213

214

215

216

217

218

219

220 Table 2. Ambient biological and cyanotoxin (microcystins) concentrations in surface waters.

221 BDL = below method detection limit.

Date	Station	Phycocyanin (µg/L)	Chlorophyll <i>a</i> (µg/L)	Dissolved MC (µg/L)	Particulate MC (µg/L)
22-Jun-15	WE6	0.155	1.63	BDL	BDL
	WE2	0.218	3.84	BDL	BDL
	WE4	0.389	1.01	BDL	BDL
20-Jul-15	WE6	0.450	2.88	BDL	BDL
	WE2	BDL	6.59	BDL	BDL
	WE4	155	120	0.150	8.46
10-Aug-15	WE6	241	353	0.150	3.10
	WE2	46.8	187	0.150	9.19
	WE4	9.89	86.3	0.280	2.29
28-Sep-15	WE6	51.8	55.0	0.340	1.99
	WE2	22.4	28.0	0.140	0.910
	WE4	17.6	22.2	0.210	0.260
19-Apr-16	WE2	–	–	–	–
30-May-16	WE4	0.36	2.60	BDL	BDL
	WE13	0.24	4.80	BDL	BDL
27-Jun-16	WE6	0.993	4.25	BDL	BDL
	WE2	0.122	4.03	BDL	BDL
	WE4	0.105	4.31	BDL	BDL
11-Jul-16	WE6	4.46	36.0	0.155	0.547
	WE2	0.453	4.14	BDL	0.137
	WE4	0.131	1.82	BDL	BDL
8-Aug-16	WE6	14.6	62.2	0.300	4.70
	WE2	4.20	39.1	0.210	3.02
	WE4	0.251	7.77	0.110	0.270
	WE13	7.79	7.20	0.140	2.27
19-Sep-16	WE6	6.02	8.80	0.280	1.41
	WE2	0.312	5.52	0.130	0.210
17-Oct-16	WE4	0.056	2.71	0.100	0.010
	WE13	0.300	8.09	0.220	0.140
	WE6	0.164	0.400	0.190	BDL
	WE2	0.239	5.20	0.150	BDL
30-May-17	WE6	0.098	2.98	BDL	BDL
	WE2	0.092	2.56	BDL	BDL
	WE4	BDL	2.45	BDL	BDL
	WE13	0.167	10.1	BDL	BDL
12-Jun-17	WE6	BDL	3.41	0.110	BDL
	WE2	0.079	26.9	0.099	BDL
	WE4	BDL	7.61	0.109	BDL
	WE13	BDL	1.94	0.250	BDL
17-Jul-17	WE6	0.103	3.25	BDL	BDL
	WE2	0.461	19.8	BDL	BDL
	WE4	BDL	2.18	0.100	BDL
	WE13	BDL	3.16	BDL	BDL
14-Aug-17	WE6	453	532	0.590	21.6
	WE2	23.2	27.1	0.140	4.00
	WE4	19.3	30.6	0.370	3.70
	WE13	2.37	12.4	0.130	0.320
18-Sep-17	WE6	19.3	33.5	0.180	0.760
	WE2	68.7	35.1	0.180	0.300
	WE4	4.75	9.62	0.230	0.250
	WE13	109	53.1	BDL	0.550
10-Oct-17	WE6	26.1	40.9	0.210	0.560
	WE2	16.8	27.7	BDL	0.450
	WE4	0.423	5.11	BDL	BDL
	WE13	9.86	14.5	BDL	0.160

222

223 Phycocyanin (cyanobacteria) and chlorophyll *a* (Table 2), followed similar patterns
224 during each year and sampling season, peaking at WE6 in August, when ambient NH_4^+
225 concentrations were at or near undetectable levels. Maximum chlorophyll *a* and phycocyanin in
226 2017 were 1.5–2 times those from the same stations in 2015, although these peak values
227 represent samples from just below the surface, not within surface scums. Chlorophyll *a* was
228 correlated with bloom day, all N forms (except NO_2^- and TN), the TN mass and N:P ratio of the
229 previous week's Maumee River load, Secchi depth, water temperature, PAR, turbidity, total
230 suspended solids, and both dissolved and particulate microcystins (Table S2). Phycocyanin was
231 similarly correlated with bloom day, all N forms (except TN), the TN mass and N:P ratio of the
232 Maumee River load from the previous week, Secchi depth, turbidity, total suspended solids, and
233 both toxin measures, but was additionally correlated with wind speed (Table S2). Particulate and
234 dissolved microcystin concentrations followed similar spatial and temporal trends in 2016 and
235 2017, with maximum values at WE6 in August. In 2015, maximum dissolved and particulate MC
236 concentrations were observed at WE6 in September and WE2 in August. In 2017, peak
237 particulate microcystins ($21.6 \mu\text{g L}^{-1}$) were measured at WE6 in August, coinciding with
238 chlorophyll *a* and phycocyanin maxima. Both dissolved and particulate microcystins were
239 correlated with bloom day, several N concentrations (NH_4^+ , NO_3^- , total dissolved N, dissolved
240 inorganic N, and particulate organic N), the TN mass of the Maumee River load from the
241 previous week, total suspended solids, chlorophyll *a*, and phycocyanin (Table S2). Neither
242 biomass nor toxin concentrations were correlated with any P form.

243 **Potential NH_4^+ uptake**

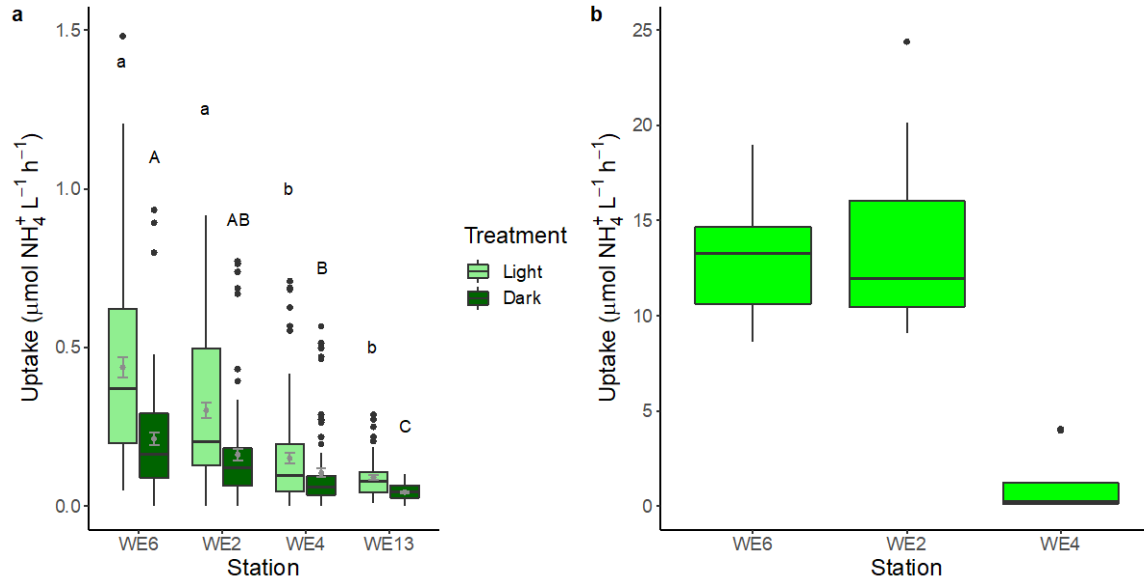
244 Potential NH_4^+ uptake rates were not influenced by depth across station ($F_{9,231} = 1.38$; $p =$
245 0.196), month ($F_{7,233} = 6.07$; $p = 0.129$), or year ($F_{3,237} = 11.8$; $p = 0.572$), so surface and bottom

246 rates were averaged. Light NH_4^+ uptake closest to the Maumee River mouth (WE6 and WE2)
247 were greater than at WE4 or WE13 ($F_{3,327} = 29.2$; $p < 0.001$), but rates at WE6 and WE2, and
248 WE4 and WE13, were not different from each other (Fig. 2a). Light NH_4^+ uptake rates were
249 different across months ($F_{6,324} = 12.8$; $p < 0.001$), with highest rates in August 2015 (Fig. 2b).
250 Disregarding August 2015, the effect of month was still robust, but August was no longer
251 different from June, July, or September ($F_{6,306} = 5.24$; $p < 0.001$; Fig. 3a). Neither spatial
252 (station) nor yearly patterns changed from adjusting linear model input. Across all months
253 (excluding August 2015), light NH_4^+ uptake was different year-to-year ($F_{2,328} = 58.8$; $p < 0.001$).
254 Uptake rates were greater in 2015 than 2016 or 2017, but light NH_4^+ uptake rates in 2016 and
255 2017 were not different from each other (Fig. 3b).

256 Dark NH_4^+ uptake rates were not different between WE2 and WE6 or WE4, but rates at
257 all of these stations were higher than WE13 ($F_{3,327} = 13.1$; $p < 0.001$; Fig. 3a). Dark NH_4^+ uptake
258 did not differ between months ($F_{6,306} = 1.14$; $p = 0.338$; Fig. 4a) and were also greater in 2015
259 than 2016 or 2017 ($F_{2,328} = 32.2$; $p < 0.001$; Fig. 3b).

260

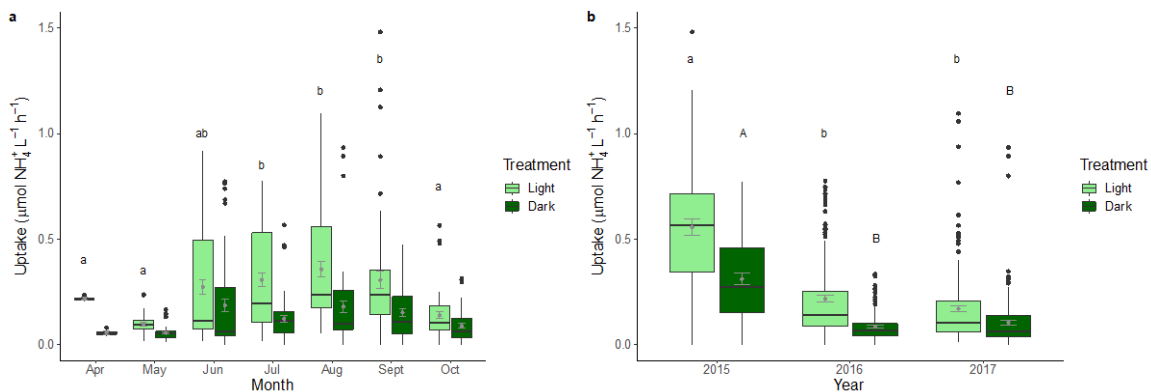
261



262

263 Figure 2. Potential NH_4^+ uptake rates ($\mu\text{mol L}^{-1} \text{h}^{-1}$) (a) in light and dark incubations across all
 264 sampling events by station, and (b) August 10, 2015 (no light/dark due to abbreviated incubation;
 265 note difference in y-axis scale). Means (\pm SE) are overlaid on each boxplot in panel (a) in gray.
 266 Letters reflect differences in uptake rates between stations (Tukey's HSD post-hoc tests) within
 267 each treatment (lowercase letters for Light, uppercase letters for Dark). n for each station: WE6 =
 268 90, WE2 = 95, WE4 = 87, WE13 = 60.

269
 270



271

272 Figure 3. (a) Potential NH_4^+ uptake rates ($\mu\text{mol L}^{-1} \text{h}^{-1}$) in the light (light green) and dark (dark
 273 green) for each month across all three years (August 2015 excluded). Means (\pm SE) are overlaid

274 on each boxplot in gray. Letters indicate differences in uptake rates between months (Tukey's
275 HSD post-hoc tests) in the light treatment; there were no differences in dark rates across months.
276 *n* for each month: April = 6, May = 36, June = 66, July = 57, August = 66, September = 53,
277 October = 48. (b) Potential NH₄⁺ uptake rates (μmol L⁻¹ h⁻¹) in the light (light green) and dark
278 (dark green) across all three years (August 2015 excluded). Means (± SE) are indicated on each
279 boxplot in gray. Letters indicate differences in uptake rates between years (Tukey's HSD post-
280 hoc tests); yearly differences in each treatment (Light and Dark) were the same. *n* for each year:
281 2015 = 71, 2016 = 117, 2017 = 144).

282

283 Excluding August, light and dark NH₄⁺ uptake rates in 2015 ranged from undetectable to
284 1.48 μmol N L⁻¹ h⁻¹ and undetectable to 0.772 μmol N L⁻¹ h⁻¹ (Figs. 3b, S1), respectively. The
285 greatest rates (light = 20.2 μmol N L⁻¹ h⁻¹, dark = 24.4 μmol N L⁻¹ h⁻¹) were observed in August
286 at WE6 and WE2. NH₄⁺ uptake rates were generally higher at these stations than at WE4 (Fig.
287 S1). In 2016, light and dark NH₄⁺ uptake rates ranged from undetectable to 0.775 μmol N L⁻¹ h⁻¹
288 and undetectable to 0.334 μmol N L⁻¹ h⁻¹, respectively (Figs. 3b, S2). Rates in 2016 peaked at
289 WE6 in July and August and WE2 in August. By October, rates had nearly returned to those
290 observed in May and June (Fig. S2). In 2017, light and dark NH₄⁺ uptake ranged from 0.011–
291 1.10 μmol N L⁻¹ h⁻¹ and undetectable to 0.934 μmol N L⁻¹ h⁻¹, respectively (Figs. 3b, S3). Rates
292 at WE6 peaked in August, which were the highest 2017 rates except WE2 in June (Fig. S3).

293 Across the entire dataset, light and dark NH₄⁺ uptake rates were correlated with many
294 physicochemical parameters, including several nutrient forms (TN, particulate organic N), both
295 biomass parameters, and microcystin concentrations (Table S2).

296 For the entire dataset, light exceeded dark NH_4^+ uptake at all stations ($F_{7,654} = 21.4$; $p <$
297 0.001), in June–October ($F_{13,648} = 9.61$; $p < 0.001$), and within each year ($F_{5,656} = 40.6$; $p <$
298 0.001). There were instances (usually WE4 and WE13) where dark NH_4^+ uptake rates were
299 comparable to or exceeded light rates, particularly in July (Figs. S1–S3).

300 NH_4^+ regeneration

301 Light and dark NH_4^+ regeneration rates were not different ($F_{1,660} = 0.637$; $p = 0.425$), so
302 they were averaged together for each incubation. Across all sampling dates, NH_4^+ regeneration
303 exhibited differences by station ($F_{3,327} = 11.8$; $p < 0.001$) and was greatest at WE6 and WE2, but
304 rates at WE6 and WE2 were not different from each other (Fig. 4a). NH_4^+ regeneration rates
305 were also different when evaluated by month ($F_{6,306} = 5.86$; $p < 0.001$), with highest regeneration
306 rates in June and July (Fig. 5a). NH_4^+ regeneration rates also varied across years ($F_{2,328} = 38.5$; p
307 < 0.001), with 2015 rates (even excluding August 2015) greater than 2016 or 2017, while the
308 latter two years were not different from each other (Fig. 5b).

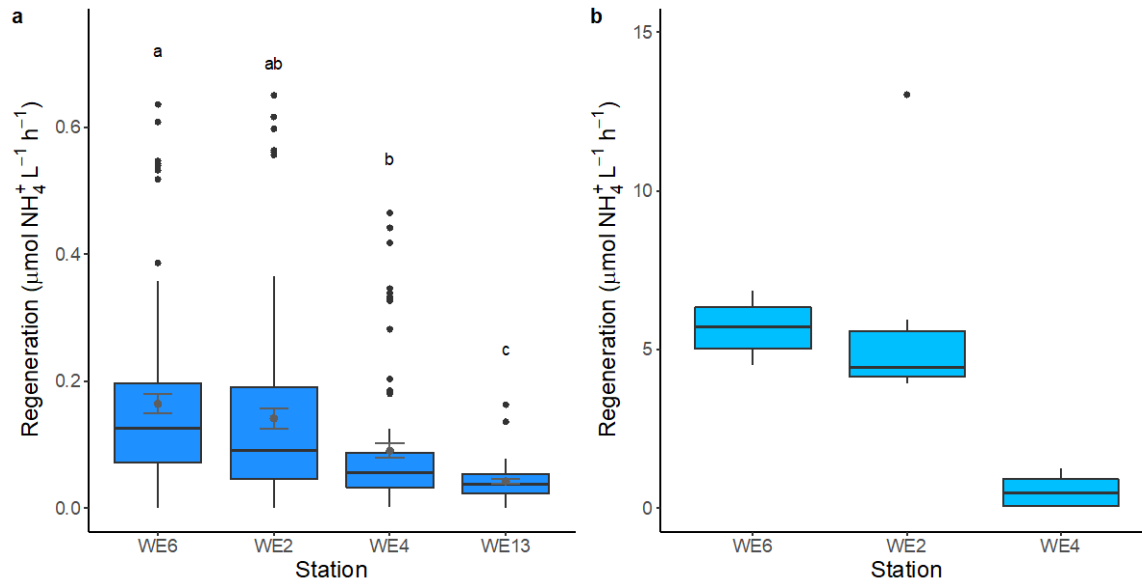
309 NH_4^+ regeneration rates peaked in August 2015 ($13.0 \mu\text{mol N L}^{-1} \text{h}^{-1}$; Fig. 4b), ranging
310 from undetectable to $0.650 \mu\text{mol N L}^{-1} \text{h}^{-1}$ across the rest of 2015 (Figs. 5b, S4). NH_4^+
311 regeneration rates in 2016 ranged from undetectable to $0.282 \mu\text{mol N L}^{-1} \text{h}^{-1}$, peaking at WE6 in
312 July and WE2 in August, before declining in September (Figs. 5b, S5). In 2017, rates ranged
313 from undetectable to $0.289 \mu\text{mol N L}^{-1} \text{h}^{-1}$ and remained low until mid-summer, reaching a
314 maximum at WE6 in August (Fig. 5b, S6).

315 NH_4^+ regeneration rates were negatively correlated with Secchi depth and positively
316 related to light and dark NH_4^+ uptake, water and air temperature, conductivity, turbidity, total
317 suspended solids, phycocyanin, chlorophyll *a*, particulate microcystins, total P, particulate
318 organic N, and TN (Table S2).

319

320

321



322

323 Figure 4. NH_4^+ regeneration rates ($\mu\text{mol L}^{-1} \text{h}^{-1}$) (a) across all months and years by sampling

324 station; and (b) from August 14, 2015 (note difference in y-axis scale). Means (\pm SE) are

325 overlaid on each boxplot in panel (a) in gray. Letters indicate differences in regeneration rates

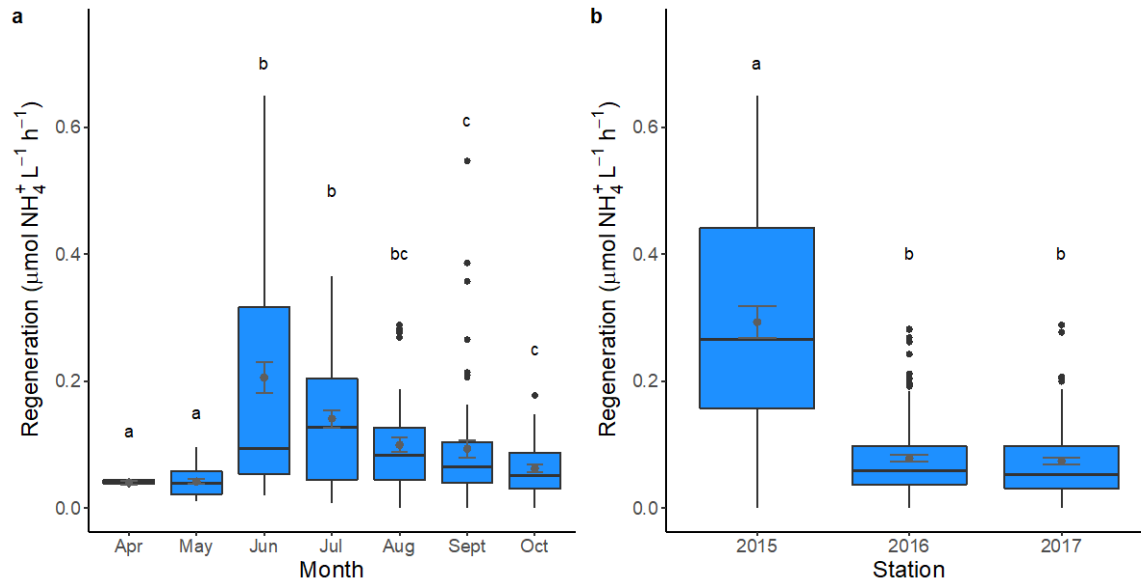
326 between sites (Tukey's HSD post-hoc tests). n for each station: WE6 = 90, WE2 = 95, WE4 =

327 87, WE13 = 60.

328

329

330



331
 332 Figure 5. (a) NH₄⁺ regeneration rates ($\mu\text{mol L}^{-1} \text{h}^{-1}$) by month across all sampling years
 333 (excluding August 2015). *n* for each month: April = 6, May = 36, June = 66, July = 57, August =
 334 66, September = 53, October = 48. (b) NH₄⁺ regeneration rates ($\mu\text{mol L}^{-1} \text{h}^{-1}$) by year (excluding
 335 August 2015). *n* for each year: 2015 = 71, 2016 = 117, 2017 = 144. Means (\pm SE) are overlaid
 336 on each boxplot in gray. Letters indicate differences in regeneration rates between (a) months or
 337 (b) years (Tukey's HSD post-hoc tests).

338
 339 The capacity of water column NH₄⁺ regeneration to support community NH₄⁺ demand in
 340 western Lake Erie exhibited similar patterns in each year, peaking in June (82.4–124%) and
 341 decreasing through August (Fig. S7a), when TN loads from the Maumee River watershed
 342 decreased (Fig. S7b). Water column nutrient concentrations (Table 1) and external TN loads
 343 (Fig. S7b) were low during peak bloom months (August and September), while NH₄⁺
 344 regeneration continued at rates supporting ~20–60% of community NH₄⁺ demand, providing an
 345 internal N load not accounted for in external loading or water column concentration
 346 measurements.

347

348 **Discussion**

349 This study (2015–2017) quantified NH_4^+ cycling rates in western Lake Erie along a
350 spatial gradient from the primary nutrient source (Maumee River) into the main basin and
351 assessed the role of internal NH_4^+ dynamics in supporting cyanoHABs. Our results explain the
352 persistence of high biomass and toxin concentrations despite N depletion.

353 **Water column NH_4^+ cycling**

354 We did not observe depth-driven differences for any rate measurement. Western Lake
355 Erie is shallow and well-mixed, and *Microcystis* can regulate buoyancy and migrate vertically in
356 the water column (Wallace et al. 2000), perhaps explaining this observation. While extreme for
357 Lake Erie, NH_4^+ regeneration and potential uptake rates measured in August 2015 were similar
358 to maxima reported during a cyanoHAB in Lake Smith, Alaska ($15.4 \mu\text{mol L}^{-1} \text{h}^{-1}$; Gu and
359 Alexander 1993). At WE6 in August 2015, extracted phycocyanin and chlorophyll *a* values from
360 surface scums were 1,700 and 1,900 $\mu\text{g L}^{-1}$, respectively (Table 3), and NH_4^+ concentrations
361 were near-undetectable (Table 1). NH_4^+ regeneration and potential uptake rates measured at a
362 station <1 km from WE6 five days prior (Fig. S8) were nearly two orders of magnitude less than
363 our highest values, but approximately half of potential NH_4^+ uptake rates at WE6 in August 2016
364 and 2017, reflecting spatial and temporal variability in bloom biomass (e.g., Chaffin et al. 2021).

365 Potential NH_4^+ uptake rates were greater in the light than dark, indicating expected
366 photoautotrophic activity when light and NH_4^+ were available. Potential NH_4^+ uptake rates across
367 both light and dark treatments were similar to, but sometimes exceeded, rates reported in other
368 eutrophic systems, including Lake Champlain (Missisquoi Bay; McCarthy et al. 2013) and Lake
369 Okeechobee (James et al. 2011), and were often much greater than those reported in Lake

370 Balaton (Présing et al. 2001), Lake Michigan (Gardner et al. 2004), Lake Superior (Kumar et al.
371 2008), and several orders of magnitude greater than those previously reported in Lake Erie
372 (Murphy 1980). In addition to differences in methodology, this large discrepancy is almost
373 certainly explained by greatly reduced phytoplankton biomass following aggressive nutrient load
374 mitigation strategies in the years prior to the study (Watson et al. 2016). Greater light NH_4^+
375 uptake rate maxima were reported in hypereutrophic Lake Taihu (Hampel et al. 2018), as well as
376 in *Planktothrix*-dominated Sandusky Bay in Lake Erie (Hampel et al. 2019a), Lake Okeechobee
377 (Hampel et al. 2019b), and subarctic Smith Lake in Alaska (Gu and Alexander 1993).

378 Maximal NH_4^+ regeneration rates in western Lake Erie were similar to those reported for
379 Lake Okeechobee (James et al. 2011) and Missisquoi Bay (Lake Champlain; McCarthy et al.
380 2013), as well as an Amazon floodplain lake (Morrissey and Fisher 1988). NH_4^+ regeneration
381 rate maxima in western Lake Erie were two orders of magnitude greater than those from Lake
382 Michigan (Gardner et al. 2004), up to an order of magnitude less than those in Sandusky Bay
383 (Hampel et al. 2019a) and Lake Okeechobee (Hampel et al. 2019b), and 3–5 times less than
384 those from Lake Taihu (McCarthy et al. 2007; Jiang et al. 2019) and Petit Saut Lake (French
385 Guyana; Collos et al. 2001). In general, NH_4^+ regeneration and potential uptake rates in this
386 study generally fell within the range of those reported for other eutrophic lakes and measured
387 using similar methods.

388 The hypothesis that community NH_4^+ uptake and turnover rates would decrease with
389 distance from the Maumee River inflow was supported by the results. WE4 and WE13 had lower
390 rates than the westernmost stations, indicating less demand and recycling further from the
391 nutrient source. We also predicted greater NH_4^+ uptake rates during peak bloom months, and
392 although there was no difference between summer months (June–September) once August 2015

393 values were disregarded, positive relationships between light NH_4^+ uptake, temperature,
394 phycocyanin, and chlorophyll *a* support this prediction.

395 Contrary to our prediction, NH_4^+ regeneration could not support potential NH_4^+ demand
396 during peak bloom periods (Fig. S7). This result agrees with findings from Lake Champlain
397 (McCarthy et al. 2013) but contrasts with *Microcystis*-dominated Lake Taihu, where summer
398 NH_4^+ regeneration rates could support 100% of community NH_4^+ demand (Hampel et al. 2018).
399 Unlike Lake Erie, NH_4^+ is detectable in Taihu in August, and the external N load is much greater
400 (Hampel et al. 2018). High NH_4^+ regeneration rates we report here represent a large, continuous
401 NH_4^+ supply to support cyanoHAB biomass and toxin production, especially during peak
402 biomass months (August and September), when cyanoHABs in Lake Erie are N-stressed
403 (Chaffin et al. 2018). N stress also decreases intracellular concentrations of N-rich microcystins
404 (Van de Waal et al. 2014). Our data suggest that toxin production during this period required
405 regenerated NH_4^+ . Sediment-water interface N effluxes also supply bioavailable N to supplement
406 water column NH_4^+ regeneration and external loading (Présing et al. 2008; McCarthy et al.
407 2016), as shown recently for the same study area of Lake Erie (Boedecker et al. 2020).

408 Throughout the study, the 2015 bloom was the most severe in terms of biomass and areal
409 coverage, followed by 2017 and 2016 (NOAA; Wynne et al. 2021; further description in
410 Supplemental Materials). Even excluding August 2015 rates, 2015 exhibited higher potential
411 NH_4^+ uptake rates than other years. N concentrations and cyanobacteria biomass were inversely
412 related (Table S2(3?)), but neither biomass proxy was related to o-PO_4^{3-} concentration. This
413 pattern reflects seasonal cyanoHAB maxima, where bioavailable N became depleted by non-N-
414 fixing *Microcystis* (Table 1). High TKN:TN ratios in the Maumee River load coincide with
415 bloom formation in mid-July, several months after spring P loads (Newell et al. 2019).

416 *Microcystis*-dominated blooms in the western basin originated in the mid-1990s (Steffen et al.
417 2014), coinciding with the increased proportion of TKN (Newell et al. 2019), while increased
418 dissolved reactive P loads did not occur until after 2002 (Jarvie et al. 2017). Combined with
419 reported over-estimation of Maumee River dissolved reactive P loads (River and Richardson
420 2019), the focus on dissolved reactive P loads as the main driver of cyanoHABs in Lake Erie
421 (e.g., Annex 4 of the Great Lakes Water Quality Agreement, IJC) is insufficient.

422 **Scaling up: NH₄⁺ regeneration in western Lake Erie**

423 CyanoHAB biomass and toxin production is sustained following N depletion by recycled
424 NH₄⁺ (McCarthy et al. 2007; Gardner et al. 2017; Hampel et al. 2018; this study). NH₄⁺
425 regeneration rates were scaled by delineating the western basin into zones by station and
426 calculating the volume of each station area (see Boedecker et al. 2020). NH₄⁺ regenerated at each
427 station was then compared to incoming TN loads from the Maumee River (NCWQR Heidelberg
428 tributary monitoring program, <https://ncwqr.org/monitoring/>, last accessed 10/17/2020; Richards
429 et al. 2010).

430 In 2015, NH₄⁺ regeneration during the sampling season added NH₄⁺ equivalent to 76% of
431 the annual TN load and 160% of the TN load during the sampling period (June–September).
432 Including August 2015, the internal NH₄⁺ regeneration load increases to 2.2 times the annual TN
433 load and 4.5 times the TN load during the sampling season. In 2016 and 2017, regenerated NH₄⁺
434 contributed NH₄⁺ equivalent to 60% of the annual TN load and 1.3–1.5 times the seasonal TN
435 load (Table 4). When monthly NH₄⁺ regeneration rates were summed to calendar year (using
436 April 2016 rates as a proxy for winter months), NH₄⁺ regeneration could supply 240–250% of
437 the annual TN load in 2016 and 2017. This relative contribution (~2×) is similar to estimates for

438 Missisquoi Bay (McCarthy et al. 2013), Lake Taihu (Hampel et al. 2018), and Sandusky Bay
 439 (~77%; Hampel et al. 2019).

440 Sediments also contribute to water column N availability in aquatic ecosystems (An and
 441 Gardner 2002; McCarthy et al. 2016). Recent work at many of the same stations as the present
 442 study reported that western basin sediments release NH_4^+ and urea at rates equivalent to 4–11%
 443 of the annual TN load (Boedecker et al. 2020). Combined, water column and sediments (NH_4^+
 444 release ~11% of water column NH_4^+ regeneration) represent a continuous supply of internal N
 445 when external N loads are minimal, cyanobacterial biomass is high, and water column N
 446 concentrations are depleted.

447

448 Table 4. Extrapolated NH_4^+ regeneration in the water column vs. annual (a) or sampling season
 449 (b) TN load (in metric tons). 2015 sampling season June–September, 2016 April–October, and
 450 2017 May–October. Regenerated NH_4^+ values in 2015 include those generated from very high
 451 rates in August.

a	Regenerated NH_4^+	TN Annual Load	% of annual load
2015	8.15×10^4	3.79×10^4	215
2016	1.64×10^4	2.72×10^4	60.3
2017	2.40×10^4	3.87×10^4	62.0

b	Regenerated NH_4^+	TN Sampling Season Load	% of seasonal load
2015	8.15×10^4	1.80×10^4	452
2016	1.64×10^4	1.05×10^4	156
2017	2.40×10^4	1.85×10^4	130

452

453 Despite high spring nutrient loading from the Maumee River, cyanoHABs do not develop
 454 in western Lake Erie until mid- or late-July, corresponding with higher water temperatures and
 455 proportion of chemically reduced N forms in the external N load (Newell et al. 2019). The ratio

456 of microcystin to phycocyanin peaked when regenerated NH_4^+ was (up to 50 times) greater than
457 the Maumee River TN load from the previous week ($F_{2,46} = 2.70$; $p = 0.020$, Fig. S9). This
458 observation suggests a ‘sweet spot’, where NH_4^+ regeneration supports biomass and toxin
459 production, and biomass maintenance is favored over toxin production (Harke and Gobler 2013).
460 When NH_4^+ regeneration exceeded weekly TN loading by > 50 times (late August and
461 September), toxin concentrations in biomass decreased and were not different from those when
462 external loads were higher than internal loading (Fig. S9).

463 Although microcystins contain, on average, 10 N per molecule (Honkanen et al. 1990),
464 there were no strong relationships between any N species and toxin concentrations in the present
465 study. Given the high rates of NH_4^+ regeneration reported here, snapshot sampling to determine
466 DIN concentrations do not accurately represent N availability. However, NH_4^+ regeneration and
467 potential uptake rates are good proxies for N demand and bioavailability (Gardner et al. 2017).
468 Thus, water column NH_4^+ cycling rates, previously missing from the literature for this and most
469 other freshwater systems, may represent key parameters to consider when developing models to
470 predict toxin concentrations in cyanoHAB impacted systems.

471 **Conclusions**

472 This study contributes to the growing body of literature highlighting the importance of
473 NH_4^+ and chemically reduced N in eutrophic lakes affected by seasonal cyanoHABs, especially
474 those comprised of non-N-fixing, toxin-producing taxa (e.g., *Microcystis*). Water column NH_4^+
475 regeneration rates met or exceeded external N loads in the western basin and help explain why
476 non-N-fixing cyanoHABs proliferate despite minimal external N loading. These results reinforce
477 the need to manage external N loading to mitigate growth and toxin production of non-N-fixing
478 cyanobacteria (e.g., McCarthy et al. 2013, 2016; Gobler et al. 2016; Newell et al. 2019). External

479 nutrient loads stimulate biomass and toxin production, which becomes the substrate for NH_4^+
480 regeneration when cells are grazed and/or remineralized in the water column (Gardner and Lee
481 1975; McCarthy et al. 2013) and sediments (McCarthy et al. 2016; Boedeker et al. 2020). Thus,
482 while in-system turnover should be accounted for in management and modeling applications,
483 reducing external nutrient loads from watersheds remains the key to mitigating the global
484 proliferation of contemporary cyanoHABs that cannot fix atmospheric N and produce N-rich
485 toxins.

486 **Acknowledgements**

487 This research was funded by Ohio Sea Grant. We thank the NOAA Great Lakes Environmental
488 Research Laboratory and the Cooperative Institute for Great Lakes Research, along with their
489 boat captains, for providing sampling opportunities aboard their vessel. We appreciate comments
490 and suggestions from colleagues at Bowling Green State University and the helpful perspective
491 on statistical approaches provided by Megan Rúa and Molly Simonis. Additional thanks to Justin
492 Chaffin at The Ohio State Stone Laboratory for sampling assistance in 2016, and to Chad
493 Hammerschmidt for his comments on early drafts. We are grateful to Justyna Hampel, Erica
494 Strope, Megan Reed, and all other Newell/McCarthy lab students and colleagues for assistance
495 with sample collection and processing.

496

497

498

499

500

501

502

503

504 **References**

505 Allinger, L.E. and Reavie, E.D., 2013. The ecological history of Lake Erie as recorded by the
506 phytoplankton community. *Journal of Great Lakes Research*, 39(3), pp.365-382.

507 An, S. and Gardner, W.S., 2002. Dissimilatory nitrate reduction to ammonium (DNRA) as a
508 nitrogen link, versus denitrification as a sink in a shallow estuary (Laguna Madre/Baffin
509 Bay, Texas). *Marine Ecology Progress Series*, 237, pp.41-50.

510 Bates, D., Maechler, M., Bolker, B., Walker, S. and Haubo Bojesen Christensen, R., 2015. lme4:
511 Linear mixed-effects models using Eigen and S4. R package version 1.1–7. 2014.

512 Bingham, M., Sinha, S.K. and Lupi, F., 2015. Economic benefits of reducing harmful algal
513 blooms in Lake Erie. *Environmental Consulting & Technology, Inc., Report*, 66.

514 Blackburn, T.H., 1979. Method for measuring rates of NH₄⁺ turnover in anoxic marine
515 sediments, using a 15N-NH₄⁺ dilution technique. *Applied and Environmental*
516 *Microbiology*, 37(4), pp.760-765.

517 Blomqvist, P., Pettersson, A. and Hyenstrand, P., 1994. Ammonium-nitrogen-A key regulatory
518 factor causing dominance of non-nitrogen-fixing cyanobacteria in aquatic
519 systems. *Archiv fur Hydrobiologie*, 132(2), pp.141-164.

520 Boedecker, A.R., Niewinski, D.N., Newell, S.E., Chaffin, J.D. and McCarthy, M.J., 2020.
521 Evaluating sediments as an ecosystem service in western Lake Erie via quantification of
522 nutrient cycling pathways and selected gene abundances. *Journal of Great Lakes*
523 *Research*, 40(4), pp.920–932.

524 Brient, L., Lengronne, M., Bertrand, E., Rolland, D., Sipel, A., Steinmann, D., Baudin, I.,
525 Legeas, M., Le Rouzic, B. and Bormans, M., 2008. A phycocyanin probe as a tool for
526 monitoring cyanobacteria in freshwater bodies. *Journal of Environmental*
527 *Monitoring*, 10(2), pp.248-255.

528 Caperon, J., Schell, D., Hirota, J. and Laws, E., 1979. Ammonium excretion rates in Kaneohe
529 Bay, Hawaii, measured by a 15 N isotope dilution technique. *Marine Biology*, 54(1),
530 pp.33-40.

531 Chaffin, J.D., Davis, T.W., Smith, D.J., Baer, M.M. and Dick, G.J., 2018. Interactions between
532 nitrogen form, loading rate, and light intensity on *Microcystis* and *Planktothrix* growth
533 and microcystin production. *Harmful Algae*, 73, pp.84-97.

534 Chaffin, J.D., Bratton, J.F., Verhamme, E.M., Bair, H.B., Beecher, A.A., Binding, C.E., Birbeck,
535 J.A., Bridgeman, T.B., Chang, X., Crossman, J. and Currie, W.J., 2021. The Lake Erie
536 HABs Grab: A binational collaboration to characterize the western basin cyanobacterial
537 harmful algal blooms at an unprecedented high-resolution spatial scale. *Harmful*
538 *Algae*, 108, p.102080.

539 Chapra, S.C. and Robertson, A., 1977. Great Lakes eutrophication: the effect of point source
540 control of total phosphorus. *Science*, 196(4297), pp.1448-1450.

541 Conroy, J.D., Kane, D.D., Dolan, D.M., Edwards, W.J., Charlton, M.N. and Culver, D.A., 2005.
542 Temporal trends in Lake Erie plankton biomass: roles of external phosphorus loading and
543 dreissenid mussels. *Journal of Great Lakes Research*, 31, pp.89-110.

544 Cooperative Institute for Great Lakes Research; University of Michigan and NOAA Great Lakes
545 Environmental Research Laboratory, 2019. Physical, chemical, and biological water
546 quality monitoring data to support detection of Harmful Algal Blooms (HABs) in western

547 Lake Erie, collected by the Great Lakes Environmental Research Laboratory and the
548 Cooperative Institute for Great Lakes Research since 2012. [2015–2017]. NOAA
549 National Centers for Environmental Information. Dataset. [https://doi.org/10.25921/11da-](https://doi.org/10.25921/11da-3x54)
550 [3x54](https://doi.org/10.25921/11da-3x54). Accessed 01-01-20.

551 Davenport, E.J., Neudeck, M.J., Matson, P.G., Bullerjahn, G.S., Davis, T.W., Wilhelm, S.W.,
552 Denny, M.K., Krausfeldt, L.E., Stough, J.M.A., Meyer, K.A. and Dick, G.J., 2019.
553 Metatranscriptomic analyses of diel metabolic functions during a *Microcystis* bloom in
554 western Lake Erie (USA). *Frontiers in Microbiology*, *10*, p.2081.

555 Davis, T.W., Harke, M.J., Marcoval, M.A., Goleski, J., Orano-Dawson, C., Berry, D.L. and
556 Gobler, C.J., 2010. Effects of nitrogenous compounds and phosphorus on the growth of
557 toxic and non-toxic strains of *Microcystis* during cyanobacterial blooms. *Aquatic*
558 *Microbial Ecology*, *61*(2), pp.149-162.

559 Davis, T.W., Bullerjahn, G.S., Tuttle, T., McKay, R.M. and Watson, S.B., 2015. Effects of
560 increasing nitrogen and phosphorus concentrations on phytoplankton community growth
561 and toxicity during *Planktothrix* blooms in Sandusky Bay, Lake Erie. *Environmental*
562 *Science & Technology*, *49*(12), pp.7197-7207.

563 Davis, T.W., Stumpf, R., Bullerjahn, G.S., McKay, R.M.L., Chaffin, J.D., Bridgeman, T.B. and
564 Winslow, C., 2019. Science meets policy: a framework for determining impairment
565 designation criteria for large waterbodies affected by cyanobacterial harmful algal
566 blooms. *Harmful algae*, *81*, pp.59-64.

567 Dolan, D.M. and McGunagle, K.P., 2005. Lake Erie total phosphorus loading analysis and
568 update: 1996–2002. *Journal of Great Lakes Research*, *31*, pp.11-22.

569 Gardner, W.S. and Lee, G.F., 1975. The role of amino acids in the nitrogen cycle of Lake
570 Mendota. *Limnology and Oceanography*, 20(3), pp.379-388.

571 Gardner, W.S., Lavrentyev, P.J., Cavaletto, J.F., McCarthy, M.J., Eadie, B.J., Johengen, T.H.
572 and Cotner, J.B., 2004. Distribution and dynamics of nitrogen and microbial plankton in
573 southern Lake Michigan during spring transition 1999–2000. *Journal of Geophysical*
574 *Research: Oceans*, 109(C3).

575 Gardner, W.S., Newell, S.E., McCarthy, M.J., Hoffman, D.K., Lu, K., Lavrentyev, P.J.,
576 Hellweger, F.L., Wilhelm, S.W., Liu, Z., Bruesewitz, D.A. and Paerl, H.W., 2017.
577 Community biological ammonium demand: a conceptual model for Cyanobacteria
578 blooms in eutrophic lakes. *Environmental Science & Technology*, 51(14), pp.7785-7793.

579 Glibert, P.M., Dennett, M.R. and Caron, D.A., 1988. Nitrogen uptake and NH₄⁺ regeneration by
580 pelagic microplankton and marine snow from the North Atlantic. *Journal of Marine*
581 *Research*, 46(4), pp.837-852.

582 Gilbert, P.M., Wilkerson, F.P., Dugdale, R.C., Raven, J.A., Dupont, C.L., Leavitt, P.R., Parker,
583 A.E., Burkholder, J.M. and Kana, T.M., 2016. Pluses and minuses of ammonium and
584 nitrate uptake and assimilation by phytoplankton and implications for productivity and
585 community composition, with emphasis on nitrogen-enriched conditions. *Limnology and*
586 *Oceanography*, 61, pp.165-197.

587 Gobler, C.J., Burkholder, J.M., Davis, T.W., Harke, M.J., Johengen, T., Stow, C.A. and Van de
588 Waal, D.B., 2016. The dual role of nitrogen supply in controlling the growth and toxicity
589 of cyanobacterial blooms. *Harmful Algae*, 54, pp.87-97.

590 Golnick, P.C., Chaffin, J.D., Bridgeman, T.B., Zellner, B.C. and Simons, V.E., 2016. A
591 comparison of water sampling and analytical methods in western Lake Erie. *Journal of*
592 *Great Lakes Research*, 42(5), pp.965-971.

593 Grömping, U., 2006. Relative importance for linear regression in R: the package
594 relaimpo. *Journal of statistical software*, 17(1), pp.1-27.

595 Gu, B. and Alexander, V., 1993. Dissolved nitrogen uptake by a cyanobacterial bloom
596 (*Anabaena flos-aquae*) in a subarctic lake. *Applied and Environmental*
597 *Microbiology*, 59(2), pp.422-430.

598 Hampel, J.J., McCarthy, M.J., Gardner, W.S., Zhang, L., Xu, H., Zhu, G. and Newell, S.E., 2018.
599 Nitrification and ammonium dynamics in Taihu Lake, China: seasonal competition for
600 ammonium between nitrifiers and cyanobacteria. *Biogeosciences*, 15(3).

601 Hampel, J.J., McCarthy, M.J., Reed, M.H. and Newell, S.E., 2019. Short term effects of
602 Hurricane Irma and cyanobacterial blooms on ammonium cycling along a freshwater–
603 estuarine continuum in south Florida. *Frontiers in Marine Science*, 6, p.640.

604 Harke, M.J. and Gobler, C.J., 2013. Global transcriptional responses of the toxic
605 cyanobacterium, *Microcystis aeruginosa*, to nitrogen stress, phosphorus stress, and
606 growth on organic matter. *PLoS One*, 8(7), p.e69834.

607 Harke, M.J., Davis, T.W., Watson, S.B. and Gobler, C.J., 2016. Nutrient-controlled niche
608 differentiation of western Lake Erie cyanobacterial populations revealed via
609 metatranscriptomic surveys. *Environmental Science & Technology*, 50(2), pp.604-615.

610 Harrell Jr, F.E., 2019. Package ‘Hmisc’. *CRAN 2019*, pp.235-6.

611 Hecky, R.E., Smith, R.E., Barton, D.R., Guildford, S.J., Taylor, W.D., Charlton, M.N. and
612 Howell, T., 2004. The nearshore phosphorus shunt: a consequence of ecosystem

613 engineering by dreissenids in the Laurentian Great Lakes. *Canadian Journal of Fisheries*
614 *and Aquatic Sciences*, 61(7), pp.1285-1293.

615 Honkanen, R.E., Zwiller, J.E.M.R., Moore, R.E., Daily, S.L., Khatra, B.S., Dukelow, M. and
616 Boynton, A.L., 1990. Characterization of microcystin-LR, a potent inhibitor of type 1 and
617 type 2A protein phosphatases. *Journal of biological chemistry*, 265(32), pp.19401-19404.

618 Hopkinson Jr, C.S., Sherr, B.F. and Ducklow, H.W., 1987. Microbial regeneration of ammonium
619 in the water column of Davies Reef, Australia. *Marine Ecology Progress Series*, pp.147-
620 153.

621 International Joint Commission (IJC), 1978. Great Lakes Water Quality Agreement.
622 <https://www.ijc.org/en/who/mission/glwqa>

623 International Joint Commission (IJC), 2018. Fertilizer Application Patterns and Trends and Their
624 Implications for Water Quality in the Western Lake Erie Basin.
625 https://legacyfiles.ijc.org/tinymce/uploaded/Publications/IJC_FertReport.pdf

626 James, R.T., Gardner, W.S., McCarthy, M.J. and Carini, S.A., 2011. Nitrogen dynamics in Lake
627 Okeechobee: forms, functions, and changes. *Hydrobiologia*, 669(1), pp.199-212.

628 Jarvie, H.P., Johnson, L.T., Sharpley, A.N., Smith, D.R., Baker, D.B., Bruulsema, T.W. and
629 Confesor, R., 2017. Increased soluble phosphorus loads to Lake Erie: Unintended
630 consequences of conservation practices?. *Journal of Environmental Quality*, 46(1),
631 pp.123-132.

632 Jiang, X., Zhang, L., Gao, G., Yao, X., Zhao, Z. and Shen, Q., 2019. High rates of ammonium
633 recycling in northwestern Lake Taihu and adjacent rivers: An important pathway of
634 nutrient supply in a water column. *Environmental pollution*, 252, pp.1325-1334.

635 Kana, T.M., Darkangelo, C., Hunt, M.D., Oldham, J.B., Bennett, G.E. and Cornwell, J.C., 1994.
636 Membrane inlet mass spectrometer for rapid high-precision determination of N₂, O₂, and
637 Ar in environmental water samples. *Analytical Chemistry*, 66(23), pp.4166-4170.

638 Kumar, S., Sterner, R.W. and Finlay, J.C., 2008. Nitrogen and carbon uptake dynamics in Lake
639 Superior. *Journal of Geophysical Research: Biogeosciences*, 113(G4).

640 Kuniyoshi, T.M., Gonzalez, A., Lopez-Gomollon, S., Valladares, A., Bes, M.T., Fillat, M.F. and
641 Peleato, M.L., 2011. 2-oxoglutarate enhances NtcA binding activity to promoter regions
642 of the microcystin synthesis gene cluster. *FEBS Letters*, 585(24), pp.3921-3926.

643 Lenth, R., Singmann, H., Love, J., Buerkner, P. and Herve, M., 2019. emmeans: Estimated
644 Marginal Means, aka Least-Squares Means (Version 1.3. 4).

645 Lumley, T. and Miller, A., 2020. Package ‘LEAPS’: Regression subset selection.

646 Martin, J.F., Kalcic, M.M., Aloysius, N., Apostel, A.M., Brooker, M.R., Evenson, G., Kast, J.B.,
647 Kujawa, H., Murumkar, A., Becker, R. and Boles, C., 2021. Evaluating management
648 options to reduce Lake Erie algal blooms using an ensemble of watershed
649 models. *Journal of Environmental Management*, 280, p.111710.

650 McCarthy, M.J., Lavrentyev, P.J., Yang, L., Zhang, L., Chen, Y., Qin, B. and Gardner, W.S.,
651 2007. Nitrogen dynamics and microbial food web structure during a summer
652 cyanobacterial bloom in a subtropical, shallow, well-mixed, eutrophic lake (Lake Taihu,
653 China). *Hydrobiologia*, 581(1), pp. 195-207).

654 McCarthy, M.J., James, R.T., Chen, Y., East, T.L. and Gardner, W.S., 2009. Nutrient ratios and
655 phytoplankton community structure in the large, shallow, eutrophic, subtropical Lakes
656 Okeechobee (Florida, USA) and Taihu (China). *Limnology*, 10(3), pp.215-227.

657 McCarthy, M.J., Gardner, W.S., Lehmann, M.F. and Bird, D.F., 2013. Implications of water
658 column ammonium uptake and regeneration for the nitrogen budget in temperate,
659 eutrophic Missisquoi Bay, Lake Champlain (Canada/USA). *Hydrobiologia*, 718(1),
660 pp.173-188.

661 McCarthy, M.J., Gardner, W.S., Lehmann, M.F., Guindon, A. and Bird, D.F., 2016. Benthic
662 nitrogen regeneration, fixation, and denitrification in a temperate, eutrophic lake: Effects
663 on the nitrogen budget and cyanobacteria blooms. *Limnology and Oceanography*, 61(4),
664 pp.1406-1423.

665 Morrissey, K.M. and Fisher, T.R., 1988. Regeneration and uptake of ammonium by plankton in
666 an Amazon floodplain lake. *Journal of Plankton research*, 10(1), pp.31-48.

667 Murphy, T.P., 1980. Ammonia and nitrate uptake in the lower Great Lakes. *Canadian Journal of*
668 *Fisheries and Aquatic Sciences*, 37(9), pp.1365-1372.

669 Newell, S.E., Davis, T.W., Johengen, T.H., Gossiaux, D., Burtner, A., Palladino, D. and
670 McCarthy, M.J., 2019. Reduced forms of nitrogen are a driver of non-nitrogen-fixing
671 harmful cyanobacterial blooms and toxicity in Lake Erie. *Harmful Algae*, 81, pp.86-93.

672 Ohio Environmental Protection Agency (OEPA), 2016. Ohio Nutrient Reduction Strategy 2015
673 Addendum. https://epa.ohio.gov/Portals/35/wqs/ONRS_addendum.pdf

674 Paerl, H.W., Scott, J.T., McCarthy, M.J., Newell, S.E., Gardner, W.S., Havens, K.E., Hoffman,
675 D.K., Wilhelm, S.W. and Wurtsbaugh, W.A., 2016. It takes two to tango: When and
676 where dual nutrient (N & P) reductions are needed to protect lakes and downstream
677 ecosystems. *Environmental Science & Technology*, 50(20), pp.10805-10813.

678 Présing, M., Herodek, S., Preston, T. and Vörös, L., 2001. Nitrogen uptake and the importance of
679 internal nitrogen loading in Lake Balaton. *Freshwater Biology*, 46(1), pp.125-139.

680 Présing, M., Spróber, P., Kovács, A.W., Vörös, L., Kenesi, G., Preston, T., Takátsy, A. and
681 Kóbor, I., 2008. Phytoplankton nitrogen demand and the significance of internal and
682 external nitrogen sources in a large shallow lake (Lake Balaton, Hungary).
683 *Hydrobiologia*, 599, pp. 87-95.

684 Puddick, J., Prinsep, M.R., Wood, S.A., Cary, S.C. and Hamilton, D.P., 2016. Modulation of
685 microcystin congener abundance following nitrogen depletion of a *Microcystis* batch
686 culture. *Aquatic Ecology*, 50(2), pp.235-246.

687 R Core Team, 2020. R: A language and environment for statistical computing. R Foundation for
688 Statistical Computing, Vienna, Austria. URL <https://www.R-project.org/>.

689 Richards, R.P., Baker, D.B., Crumrine, J.P. and Stearns, A.M., 2010. Unusually large loads in
690 2007 from the Maumee and Sandusky Rivers, tributaries to Lake Erie. *Journal of Soil
691 and Water Conservation*, 65(6), pp.450-462.

692 River, M. and Richardson, C.J., 2019. Dissolved reactive phosphorus loads to western Lake Erie:
693 The hidden influence of nanoparticles. *Journal of environmental quality*, 48(3), pp.645-
694 653.

695 Sayers, M.J., Grimm, A.G., Shuchman, R.A., Bosse, K.R., Fahnenstiel, G.L., Ruberg, S.A. and
696 Leshkevich, G.A., 2019. Satellite monitoring of harmful algal blooms in the Western
697 Basin of Lake Erie: A 20-year time-series. *Journal of Great Lakes Research*, 45(3),
698 pp.508-521.

699 Smith, D.J., Tan, J.Y., Powers, M.A., Lin, X.N., Davis, T.W., Dick, G.J., 2021. Individual
700 *Microcystis* colonies harbor distinct bacterial communities that differ by *Microcystis*
701 oligotype and with time. *Environmental Microbiology*, 23, 3020-3036,
702 <https://doi.org/10.1111/1462-2920.15514>.

703 Steffen, M.M., Li, Z., Effler, T.C., Hauser, L.J., Boyer, G.L. and Wilhelm, S.W., 2012.
704 Comparative metagenomics of toxic freshwater cyanobacteria bloom communities on
705 two continents. *PloS One*, 7(8), p.e44002.

706 Steffen, M.M., Belisle, B.S., Watson, S.B., Boyer, G.L. and Wilhelm, S.W., 2014. Status, causes
707 and controls of cyanobacterial blooms in Lake Erie. *Journal of Great Lakes*
708 *Research*, 40(2), pp.215-225.

709 Stumpf, R.P., Johnson, L.T., Wynne, T.T. and Baker, D.B., 2016. Forecasting annual
710 cyanobacterial bloom biomass to inform management decisions in Lake Erie. *Journal of*
711 *Great Lakes Research*, 42(6), pp.1174-1183.

712 Takamura, N., Iwakuma, T. and Yasuno, M., 1987. Uptake of ¹³C and ¹⁵N (ammonium, nitrate
713 and urea) by *Microcystis* in Lake Kasumigaura. *Journal of Plankton Research*, 9(1),
714 pp.151-165.

715 United States Environmental Protection Agency (USEPA), 2015. Preventing Eutrophication:
716 Scientific Support for Dual Nutrient Criteria.
717 <https://www.epa.gov/sites/production/files/documents/nandpfactsheet.pdf>

718 Van de Waal, D.B., Smith, V.H., Declerck, S.A., Stam, E.C. and Elser, J.J., 2014. Stoichiometric
719 regulation of phytoplankton toxins. *Ecology letters*, 17(6), pp.736-742.

720 Watson, S.B., Miller, C., Arhonditsis, G., Boyer, G.L., Carmichael, W., Charlton, M.N.,
721 Confesor, R., Depew, D.C., Höök, T.O., Ludsin, S.A. and Matisoff, G., 2016. The re-
722 eutrophication of Lake Erie: Harmful algal blooms and hypoxia. *Harmful algae*, 56,
723 pp.44-66.

724 Wynne, T.T., Stumpf, R.P., Tomlinson, M.C., Fahnenstiel, G.L., Dyble, J., Schwab, D.J. and
725 Joshi, S.J., 2013. Evolution of a cyanobacterial bloom forecast system in western Lake
726 Erie: development and initial evaluation. *Journal of Great Lakes Research*, 39, pp.90-99.

727 Wynne, T.T., Stumpf, R.P., Litaker, R.W. and Hood, R.R., 2021. Cyanobacterial bloom
728 phenology in Saginaw Bay from MODIS and a comparative look with western Lake
729 Erie. *Harmful Algae*, 103, p.101999.

730 Yin, G., Hou, L., Liu, M., Liu, Z. and Gardner, W.S., 2014. A novel membrane inlet mass
731 spectrometer method to measure $^{15}\text{NH}_4^+$ for isotope-enrichment experiments in aquatic
732 ecosystems. *Environmental Science & Technology*, 48(16), pp.9555-9562.

733